© 2017. Published by The Company of Biologists Ltd | Development (2017) 144, 4604-4615 doi:10.1242/dev.150110

RESEARCH ARTICLE

Neuronal LRP4 regulates synapse formation in the developing CNS

Andromachi Karakatsani[1,2,3], Nicolás Marichal[4,5,*], Severino Urban[2,3,*], Georgios Kalamakis[6], Alexander Ghanem[7], Anna Schick[1], Yina Zhang[1], Karl-Klaus Conzelmann[7], Markus A. Rüegg[8], Benedikt Berninger[4,5], Carmen Ruiz de Almodovar[2,3], Sergio Gascón[1,9,10,‡,§] and Stephan Kröger[1,‡,§]

ABSTRACT

The low-density lipoprotein receptor-related protein 4 (LRP4) is essential in muscle fibers for the establishment of the neuromuscular junction. Here, we show that LRP4 is also expressed by embryonic cortical and hippocampal neurons, and that downregulation of LRP4 in these neurons causes a reduction in density of synapses and number of primary dendrites. Accordingly, overexpression of LRP4 in cultured neurons had the opposite effect inducing more but shorter primary dendrites with an increased number of spines. Transsynaptic tracing mediated by rabies virus revealed a reduced number of neurons presynaptic to the cortical neurons in which LRP4 was knocked down. Moreover, neuron-specific knockdown of LRP4 by *in utero* electroporation of LRP4 miRNA *in vivo* also resulted in neurons with fewer primary dendrites and a lower density of spines in the developing cortex and hippocampus. Collectively, our results demonstrate an essential and novel role of neuronal LRP4 in dendritic development and synaptogenesis in the CNS.

KEY WORDS: LRP4, Central nervous system development, Synapse formation, Dendritogenesis, Transsynaptic tracing, Agrin, *In utero* electroporation, PSD95, Bassoon, Mouse

INTRODUCTION

During the last few decades we have acquired substantial knowledge on how neuromuscular junctions (NMJs) are formed in the peripheral nervous system (PNS; for a review, see Tintignac et al., 2015). Conversely, the molecular determinants orchestrating synapse formation in the central nervous system (CNS) are complex and much less understood. Although the molecular cascades governing synaptogenesis in the CNS and the PNS seem to be fundamentally different, the existence of organizational proteins common to both types of synapses suggests that the development of both structures might share several common pathways.

A key regulator for NMJ development is the low-density lipoprotein receptor-related protein 4 (LRP4; Weatherbee et al., 2006; Wu et al., 2012; Yumoto et al., 2012). At the NMJ, LRP4 forms a complex with the muscle-specific tyrosine kinase MuSK in the muscle fiber plasma membrane; this complex serves as the receptor for the motoneuron-derived extracellular matrix protein agrin (Kim et al., 2008; Zhang et al., 2008). Binding of agrin to the tetrameric LRP4/MuSK complex activates an intracellular signaling cascade in the muscle fiber resulting in the formation of most, if not all, postsynaptic specializations (Tintignac et al., 2015). LRP4 can also act as a muscle-derived retrograde stop signal for motor axons and promote the formation of presynaptic specializations at the NMJ (Wu et al., 2012; Yumoto et al., 2012). Although motoneurons also express LRP4, the functions of neuron-derived LRP4 at the NMJ are not fully understood.

In addition to the PNS, LRP4 plays crucial roles in the adult CNS, including maintenance of excitatory synaptic transmission, hippocampal synaptic plasticity, fear conditioning, associative and spatial learning, and long-term potentiation (Gomez et al., 2014; Pohlkamp et al., 2015; Sun et al., 2016). Accordingly, *Lrp4* mRNA is present in the neocortex, hippocampus, cerebellum and olfactory bulb (Lein et al., 2007; Sun et al., 2016; Tian et al., 2006). Moreover, LRP4 protein has been detected in postsynaptic membrane fractions purified from adult rat forebrain where it interacts with the postsynaptic scaffold protein PSD95 (also known as DLG4) (Gomez et al., 2014; Tian et al., 2006). Recently, astrocyte-expressed LRP4 activated by agrin has been shown to modulate glutamatergic synaptic transmission by regulating the release of ATP from astrocytes (Sun et al., 2016). Although these data show a requirement of astroglial LRP4 for normal function of the adult brain, it is still unknown whether LRP4 regulates synaptogenesis in the developing CNS in a similar way as at the NMJ.

In this study, we investigated the effects of increased or decreased expression of LRP4 on cultured CNS neurons as well as on neurons in mouse cortex and hippocampus *in vivo*. We show a crucial role for neuronal LRP4 activated by agrin in the developing CNS during dendritic development and synapse formation.

RESULTS

Expression levels of LRP4 in cultured neurons determine the shape of dendritic arbors, the number of primary dendrites and the density of dendritic spines

To begin to examine LRP4 in CNS neurons, we investigated its expression using dissociated cells from the embryonic cerebral

[1]Department of Physiological Genomics, Ludwig-Maximilians-University, Grosshaderner Str. 9, D-82152 Planegg-Martinsried, Germany. [2]Biochemistry Center (BZH), Heidelberg University, 69120 Heidelberg, Germany. [3]Interdisciplinary Center for Neurosciences, Heidelberg University, 69120 Heidelberg, Germany. [4]Institute of Physiological Chemistry, University Medical Center of the Johannes Gutenberg University Mainz, Hanns-Dieter-Hüsch Weg 19, D-55128 Mainz, Germany. [5]Focus Program Translational Neurosciences Mainz, Johannes Gutenberg University Mainz, Langenbeckstrasse 1, D-55131 Mainz, Germany. [6]Division of Molecular Neurobiology, German Cancer Research Center (DKFZ), 69120 Heidelberg, Germany. [7]Max von Pettenkofer Institute and Gene Center, Ludwig-Maximilians-University, D-81377, Munich, Germany. [8]Biozentrum, University of Basel, 4056 Basel, Switzerland. [9]Institute for Stem Cell Research, Helmholtz Center Munich at the Biomedical Center (BMC), Grosshaderner Strasse 9, D-82152 Planegg-Martinsried, Germany. [10]Toxicology and Pharmacology Department, Faculty of Veterinary Medicine, Complutense University, Ave. Puerta de Hierro s/n, 28040 Madrid, Spain.
*These authors contributed equally to this work
‡These authors contributed equally to this work

[§]Authors for correspondence (sergio.gascon@med.uni-muenchen.de; skroeger@lmu.de)

S.G., 0000-0001-8756-7082; S.K., 0000-0002-4626-1690

Received 1 February 2017; Accepted 11 October 2017

Development (2017) 144, 4604-4615 doi:10.1242/dev.150110

cortex and hippocampus at different days *in vitro* (DIV3, 6, 8, 10 and 12) with two independently generated antibodies against LRP4 (see Materials and Methods). Cultures were co-labeled with antibodies against microtubule-associated protein 2 (MAP2), which localizes to the soma and the dendrites of neurons (Caceres et al., 1984). We detected LRP4 immunoreactivity in cortical and hippocampal neurons at all stages analyzed (Fig. 1A). In particular, we observed abundant punctate LRP4 staining in neuronal cell bodies (Fig. 1Ba,Ba′) and in the proximal MAP2-positive dendrites (Fig. 1Bb,Bb′). Staining was also evident in axons as well as dendritic and axonal growth cones (Fig. 1Bb,Bb′, insets with one and two asterisks; Fig. 1C). Immunostaining of hippocampal neurons with antibodies for LRP4 and either CamKII (Jones et al., 1994) or GABA (Sloviter and Nilaver, 1987) demonstrated the presence of LRP4 in both excitatory and inhibitory neurons, respectively (Fig. S1). The specificity of the LRP4 antibodies used for immunocytochemistry was confirmed by western blotting, where a single band with an apparent molecular mass of 250 kDa was detected in cultured astrocytes, as previously described (Sun et al., 2016), as well as extracts from cultured embryonic neurons (Fig. 1D). Collectively, these results demonstrate the presence of LRP4 in embryonic neurons.

To investigate the role of LRP4 in embryonic neurons, in particular to determine if its expression influences the establishment of the neuronal network, we examined the effect of LRP4 knockdown and overexpression in cultured CNS neurons. To reduce LRP4 expression we used two different synthetic microRNAs (miR1232 and miR1544), both targeting the open reading frame of *Lrp4* mRNA. Both microRNAs were selected based on their efficacy in reducing LRP4 levels (see Materials and Methods; Fig. S2A,B) and were cloned in tandem into a single vector together with the DsRed cDNA under the control of a CAG promoter (pCAG-miRLRP4-DsRed; Fig. S2B). As control, we used the pCAG-DsRed vector lacking both microRNA sequences (Fig. S2B). Primary cortical and hippocampal neurons were co-transfected at DIV3 with a cDNA encoding a synapsin-driven eGFP:actin fusion protein (SYN-GFP:actin) in combination with either the pCAG-miRLRP4-DsRed or with the pCAG-DsRed vector. The pSYN-GFP:actin expression allowed a detailed analysis of neuronal processes and dendritic spines in the transfected cells (Fischer et al., 1998) that were analyzed 7-9 days post-transfection (DPT). The LRP4 expression levels and the morphology of neurons transfected with the control plasmids were indistinguishable from non-transfected neurons (Fig. S2B,C; data not shown), demonstrating that neither the transfection nor the expression of either GFP:actin or DsRed influence the normal phenotype of cultured neurons. In contrast, transfection with the pCAG-miRLRP4-DsRed vector led to a severe reduction of LRP4 immunoreactivity (Fig. S2B), providing additional evidence for the specificity of the anti-LRP4 antibodies. Knockdown of LRP4 resulted in a noticeable increase of the length of the primary dendrites in both cortical and hippocampal neurons (Fig. 2A;

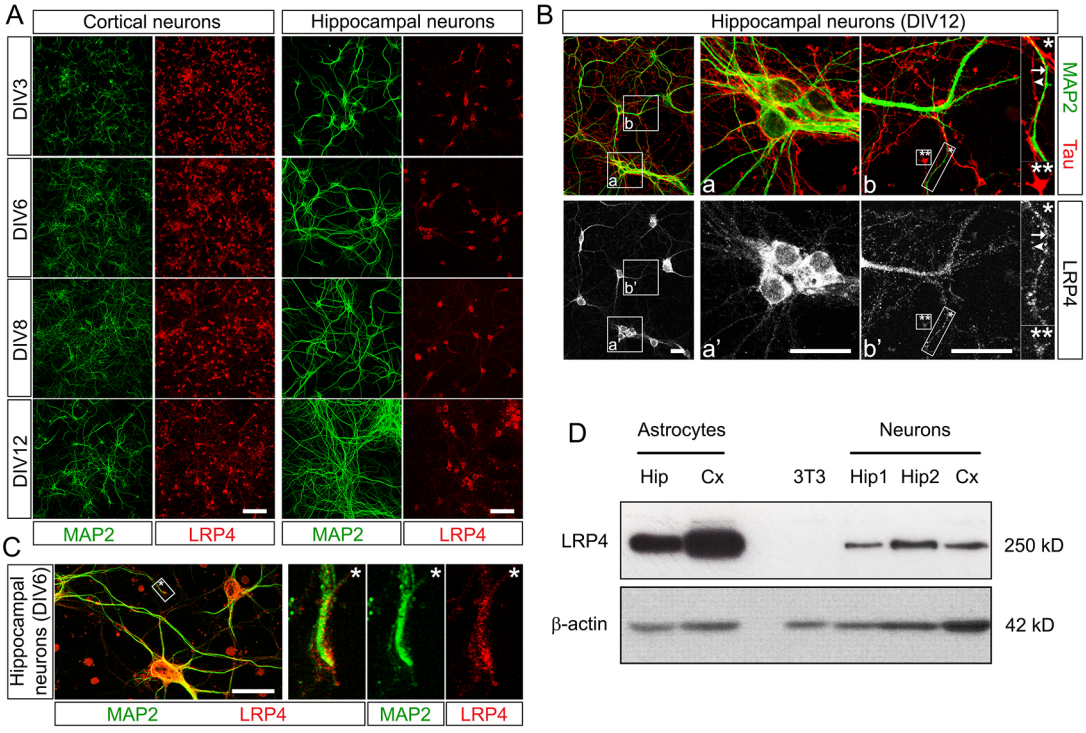

Fig. 1. LRP4 expression in cultures from embryonic cerebral cortex and hippocampus. (A) Developmental analysis of dissociated cells from E14 cerebral cortex and hippocampus double-labeled for LRP4 (red channel) and MAP2 (green channel). Note that LRP4 is associated with neurons at all stages analyzed (DIV3, 6, 8 and 12). (B) Dissociated cells from E16 embryonic hippocampus at DIV12, labeled for LRP4, MAP2 and Tau. Note that LRP4 is localized in the dendrites (white box with one asterisk in b,b′, arrow) and the axons (white box with one asterisk in b,b′, arrowhead), as well as in growth cones (white box with two asterisks in b,b′). Strong expression of LRP4 was also detected around the cell bodies of hippocampal neurons (a,a′). (C) Dissociated cells from E16 hippocampus fixed on DIV6 and labeled for LRP4 and MAP2. Note that LRP4 is also localized in dendritic growth cones (inset with one asterisk). (D) Western blotting of protein lysates from two independent hippocampal neuron (Hip) preparations and a cortical neuron (Cx) preparation probed with anti-LRP4 antibodies and anti-β-actin antibodies (lower panel) as loading control. Lysates from astroglial cells derived from cortex and hippocampus were used as positive controls, whereas lysates from NIH3T3 fibroblasts (3T3) were used as negative controls in order to determine the specificity of the antisera. The antibodies reacted with a single band of 250 kDa, corresponding to the molecular mass of LRP4. Scale bars: 100 µm (A); 50 µm (B,C, main panels); 25 µm (Ba,Ba′,Bb,Bb′).

Development (2017) 144, 4604-4615 doi:10.1242/dev.150110

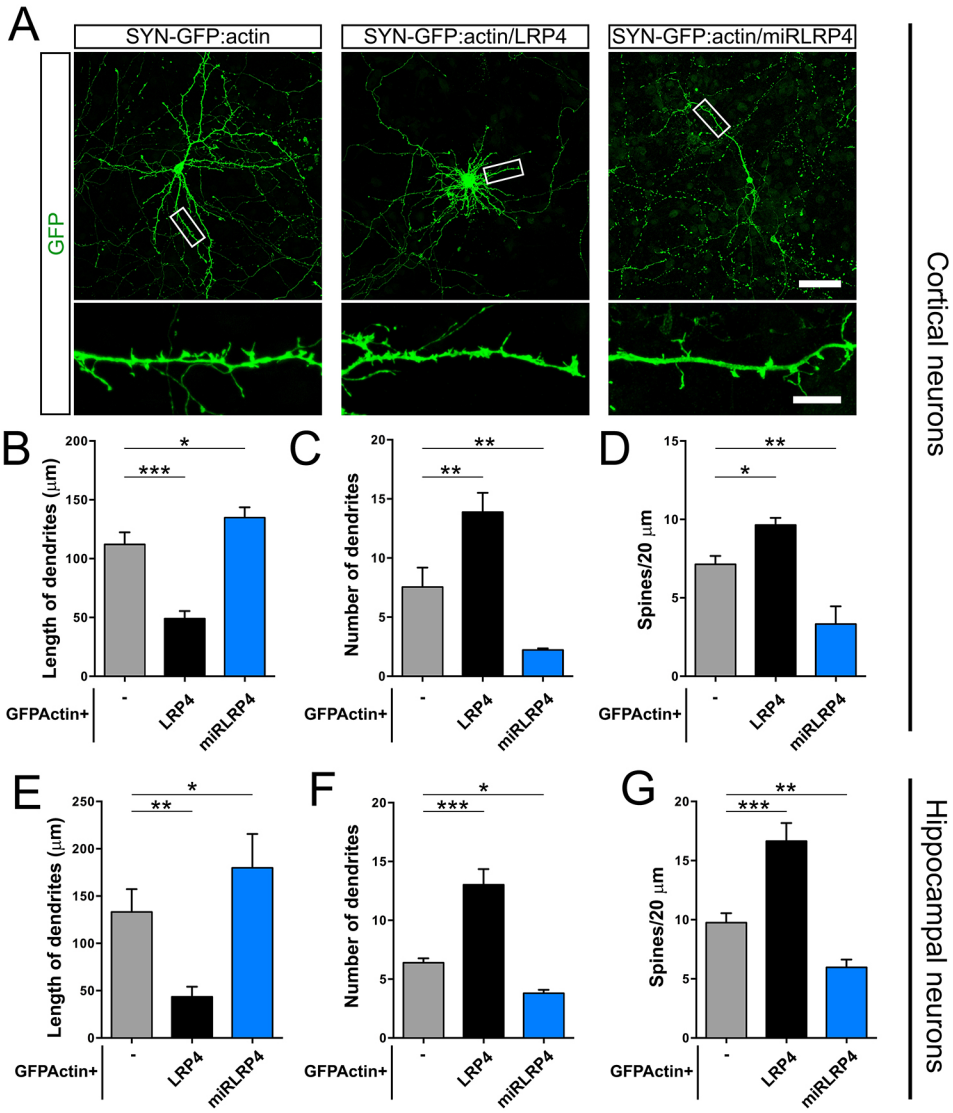

Fig. 2. LRP4 affects the number and length of dendrites and the number of spines in cultured cortical and hippocampal neurons. (A) Representative examples of dissociated cells from E14 cerebral cortex at DIV10 co-transfected with pSYN-GFP:actin together with either pCAG-miRLRP4 or pSYN-LRP4 at DIV3. Enlarged images of dendritic segments are shown to illustrate the dendritic spines. (B-G) Quantifications of the average length of the primary dendrites (B,E), number of primary dendrites (C,F) and density of spines (D,G) in cortical (upper panels) and hippocampal (lower panels) neurons. Note that overexpression of LRP4 significantly increased the number of primary dendrites (C,F; black bars) and the density of spines (D,G; black bars) and decreased the average dendritic length (B,E; black bars) in both cortical and hippocampal neurons. In contrast, knockdown of LRP4 significantly decreased the number of primary dendrites (C,F; blue bars) and spines (D,G; blue bars) and significantly increased the average dendritic length in cortical (B; blue bar) and hippocampal (E; blue bar) neurons. Data are shown as mean±s.d. from three independent experiments, *n*=15-25 cortical neurons per condition/experiment; *n*=5-10 hippocampal neurons per condition/experiment. **P*<0.05, ***P*<0.01, ****P*<0.001 (one-way ANOVA with Dunnett's post-hoc test). Scale bars: 50 µm (A, main panels); 10 µm (A, insets).

Fig. 2B,E, blue bars). Additionally, reduced LRP4 expression led to a decrease in the number of primary dendrites extending from the neuron soma (Fig. S2B; Fig. 2A; Fig. 2C,F, blue bars) and the density of spines (Fig. 2D,G, blue bars). These results demonstrate that reduced levels of LRP4 affect number of dendritic processes, dendritic length and density of spines in cultured cortical and hippocampal neurons.

We hypothesized that increased levels of LRP4 might induce the opposite phenotype compared with the effect of the miRNAs. To investigate this, cortical and hippocampal neurons were co-transfected at DIV3 with a vector encoding LRP4 under the control of the neuron-specific human synapsin promoter (pSYN-LRP4) and the SYN-GFP:actin vector. Recombinant LRP4 was exclusively expressed in neurons as predicted by the synapsin promoter (Gascón et al., 2008; Kügler et al., 2001; Fig. S2C). Morphometric analysis of the dendritic structure revealed a significant decrease in the length of primary dendrites of both cortical (Fig. 2A; Fig. 2B, black bar) and hippocampal (Fig. 2E, black bar) neurons overexpressing LRP4 compared with neurons transfected with the control vector (Fig. 2A; Fig. 2B,E, gray bars). We also observed an increased number of primary dendritic processes and density of spines in hippocampal and cortical neurons transfected with the LRP4-encoding vector (Fig. 2A; Fig. 2C,D,F, G, black bars). Thus, reduced expression of LRP4 in embryonic neurons increased the overall length of primary dendrites and decreased the number of dendrites and spines, whereas increased levels of LRP4 expression had the opposite effect on dendritic number and length, as well as density of dendritic spines.

LRP4 levels influence the shape of dendritic arbors prior to affecting the density of dendritic spines

Previous studies demonstrated that in *Lrp4*$^{-/-}$ mice the α-motoneuron growth cone continues to grow along the muscle fiber and fails to develop into a presynaptic terminal (Weatherbee et al., 2006). As a consequence, axons with deficient capacity to establish synapses might become unusually long. This suggests that the dendritic phenotype observed upon altered LRP4 levels might be secondary to differences in synaptic density at the CNS. To test this hypothesis, we analyzed the progressive development of spines and dendrites in cultured neurons with increased and reduced levels of LRP4 at different time points. We first focused on the early stages of development (DIV3-8), when dendrites are almost devoid of mature spines and synapses. Interestingly, upon LRP4 overexpression, both hippocampal and cortical neurons exhibited

Development (2017) 144, 4604-4615 doi:10.1242/dev.150110

reduced length and increased number of primary dendritic processes already at DIV6 (Fig. 3A, top; Fig. 3B,C). In contrast, neither hippocampal nor cortical neurons overexpressing LRP4 displayed changes in the density of spines at DIV6 (Fig. 3D). Likewise, the number of dendrites was significantly reduced upon LRP4 knockdown in hippocampal neurons at DIV8, prior to the reduction of spine density (Fig. 3D, left). Thus, these data indicate that the effect of LRP4 on dendritic arborization takes place before the development of synaptic specializations.

Interestingly, we observed that, whereas the differences in the dendritic length and spine density induced upon LRP4 overexpression and knockdown were maintained or even increased over time (from DIV3 to DIV21; Fig. 3B,D), the early effect on dendritic number (DIV6 to DIV12; Fig. 3C) became milder or disappeared during the maturation period (DIV12 to DIV21; Fig. 3C). Thus, at DIV21 we did not observe statistical differences in the number of dendrites in cortical and hippocampal neurons transfected with either the control or the miRNA-encoding plasmids (Fig. 3C). This suggests that the phenotype induced by altered levels of LRP4 on spine density and dendritic length is persistent, whereas the changes in dendritic numbers are rather transient.

To investigate further the mechanism by which LRP4 regulates dendritic development we followed the dynamics of neurite growth by time-lapse video microscopy (Fig. S3). As expected, control neurons exhibited extensive changes in the dendritic length over the tracking time period. Some dendrites decreased in length; however, the majority of them increased. In contrast, upon LRP4 overexpression neither shrinkage nor growth was observed, indicating that LRP4 expression diminishes growth cones'

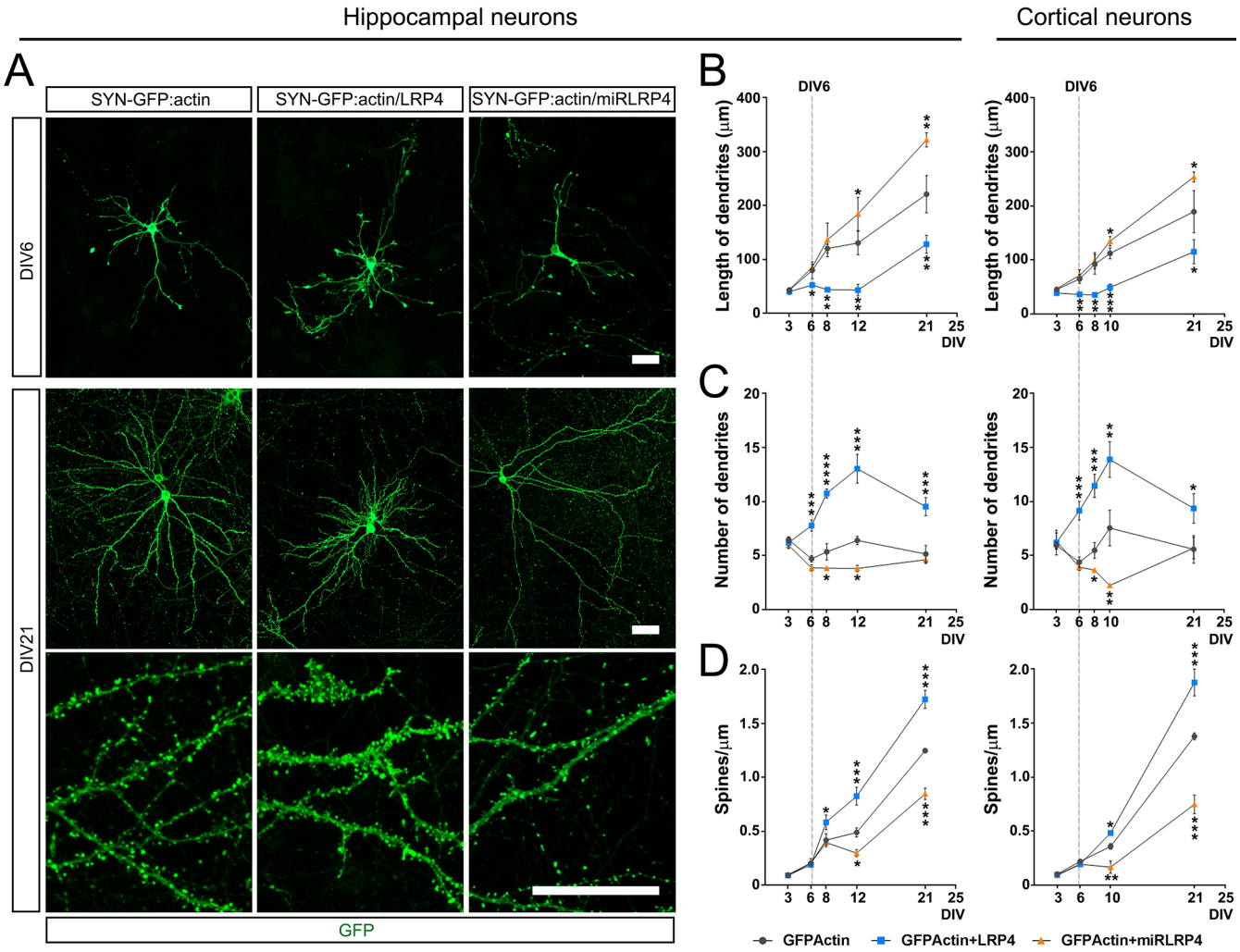

Fig. 3. LRP4 levels influence the shape of dendritic arbors during development. (A) Representative examples of dissociated cells from E16 hippocampus at DIV6 and DIV21 co-transfected with pSYN-GFP:actin and either pSYN-LRP4 or pCAG-miRLRP4. Enlarged images of dendritic segments are shown to illustrate the dendritic spines at DIV21. (B-D) Quantifications of the average length of the primary dendrites (B), number of primary dendrites (C) and density of spines (D) in hippocampal (left panels) and cortical (right panels) neurons over time (days *in vitro*). A dashed line has been placed to indicate the time point DIV6 for all the graphs. Note that overexpression of LRP4 significantly increased the number of primary dendrites (C; blue points) and decreased their length (B; blue points) already at DIV6 in both hippocampal and cortical neurons, whereas the increase in the density of spines (D; blue points) was evident at later stages (DIV8 in hippocampal neurons and DIV10 in cortical neurons). In contrast, knockdown of LRP4 significantly decreased the number of primary dendrites in both cell types already at DIV8 (C; orange points), whereas the effects on dendritic length (B) and density of spines (D) were evident at later developmental stages (DIV12 in hippocampal neurons and DIV10 in cortical neurons). Data are shown as mean±s.d. from three independent experiments, n=5-10 cortical neurons per condition/experiment; n=5-10 hippocampal neurons per condition/experiment. *P<0.05, **P<0.01, ***P<0.001 (one-way ANOVA with Dunnett's post-hoc test). Scale bars: 50 µm (A, top and middle rows); 10 µm (A, bottom row).

Development (2017) 144, 4604-4615 doi:10.1242/dev.150110

extension and retraction dynamics, which ultimately results in a reduced dendritic length. This suggests that LRP4 might regulate molecular pathways involved in the elongation or retraction of dendrites, which is in concordance with the expression of LRP4 in dendritic growth cones (Fig. 1C).

LRP4 levels affect the formation of synapse-like specializations

Our previous observations suggested that LRP4 expression levels affect the formation of synaptic specializations. To scrutinize this hypothesis further, we first examined whether knocking down LRP4 in CNS neurons was accompanied by a decrease in the density of puncta labeled by antibodies against pre- and postsynaptic marker proteins. In both hippocampal and cortical neurons, the density of puncta labeled by antibodies against the presynaptic proteins bassoon and synaptobrevin-2 (VAMP2) was significantly decreased (Fig. 4A; Fig. 4B,D, blue bars). We also observed a small reduction in the density of puncta labeled by an antibody against the postsynaptic protein PSD95, although this was not statistically significant (Fig. 4A; Fig. 4C, blue bar). Overall, these results demonstrate that reducing the amount of endogenous LRP4 leads to a decrease in the number of synapses in embryonic neurons.

We next investigated whether the number of synaptic puncta was increased upon LRP4 overexpression. In hippocampal and cortical neurons transfected with the LRP4-encoding vector, we observed an increase in the number of bassoon- (Fig. 4A; Fig. 4B, black bar) and synaptobrevin-2- (Fig. 4D, black bar) positive puncta. Likewise, the number of PSD95-positive puncta was also increased in hippocampal neurons (Fig. 4A; Fig. 4C, black bar). Taken together, these results demonstrate that an increase of LRP4 levels affected the density of synapse-like specializations in CNS neurons

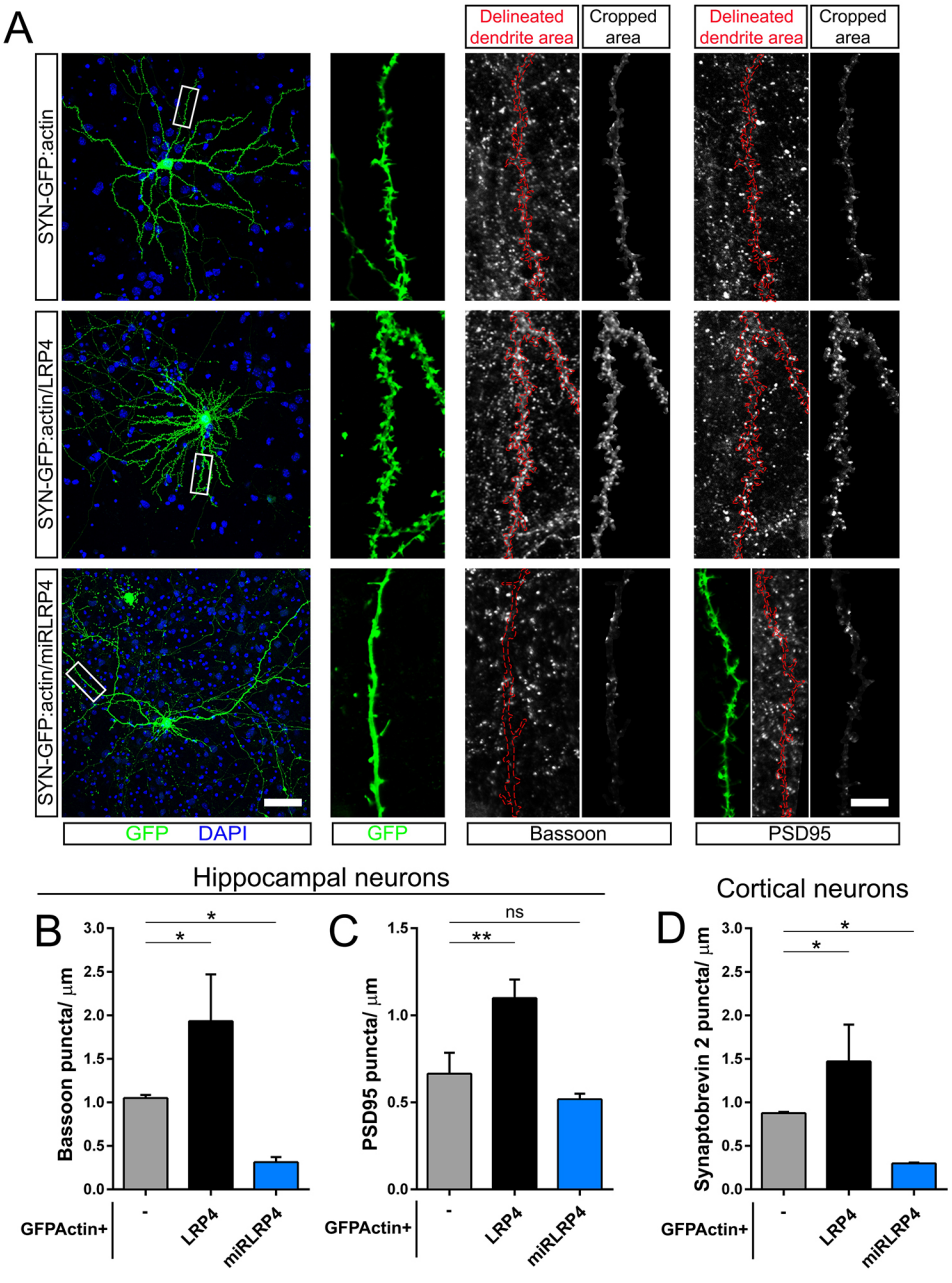

Fig. 4. LRP4 affects the number of pre- and postsynaptic specializations in neuronal cultures. (A) Representative examples of dissociated cells from E16 hippocampus co-transfected with pSYN-GFP:actin and either pSYN-LRP4 or pCAG-miRLRP4. Enlarged images of single confocal planes of individual dendritic segments are shown. The dendrite was re-drawn in red from the GFP signal in order to visualize the close association of the dendritic spines and the bassoon- and PSD95-positive puncta, respectively. Note that changes in the expression levels of LRP4 affected the number of pre- and post-synaptic puncta. The number of synapse-like specializations was only altered in the dendrites of the transfected neurons. The cropped areas show the synaptic specializations directly overlapping with the dendrite of the transfected cell (as indicated by the red line) without the synaptic specializations of the surrounding area (representing non-transfected neurons). This allowed us to distinguish the synaptic specializations directly associated with the dendrite of the transfected neurons from those of non-transfected ones and represents a more direct visualization of the number of synaptic specializations associated with a particular dendritic segment.
(B-D) Quantitative analysis of the number of bassoon- (B) and PSD95- (C) positive puncta associated with the dendrites of hippocampal neurons and the number of synaptobrevin-2-positive puncta (D) associated with the dendrites of cortical neurons revealed a significant increase of bassoon (B; black bar), PSD95 (C; black bar) and synaptobrevin-2 (D; black bar) in all neurons upon LRP4 overexpression. In contrast, knockdown of LRP4 led to a significant decrease in the number of bassoon- (B; blue bar) and synaptobrevin-2- (D; blue bar) positive puncta, without affecting the number of PSD95-positive puncta (C; blue bar). Data show mean±s.d. from three independent experiments with 5-7 cortical and 5-8 hippocampal neurons per condition/experiment. **P*<0.05, ***P*<0.01 (one-way ANOVA test with Dunnett's post-hoc test); ns, not significant. Scale bars: 50 µm.

Development (2017) 144, 4604-4615 doi:10.1242/dev.150110

in vitro. Overall, our results demonstrate that both dendritic morphology and density of synapse-like specializations on dendrites are modulated by expression levels of LRP4 in cultured cortical and hippocampal neurons.

Knockdown of LRP4 reduces the number of direct presynaptic partners in neuronal cultures

Our results so far demonstrated that LRP4 knockdown significantly reduced the number of dendritic spines and synapse-like specializations in hippocampal and cortical neurons (Figs 2-4). To investigate the extent to which these alterations affect functional synaptic connectivity, we next analyzed the spontaneous miniature excitatory postsynaptic currents (mEPSCs) in neurons transfected with the plasmid encoding the LRP4 miRNAs. Although we observed a reduction in the frequency and amplitude of mEPSCs upon LRP4 knockdown (Fig. S4), the differences were not statistically significant, probably owing to the high variability among neurons in the control cultures. Furthermore, changes in frequency of mEPSCs are not always proportional to the number of synapses, as changes in the stochastic release of presynaptic neurotransmitters or density of postsynaptic receptors could affect the mEPSC values as well. Thus, to further examine whether LRP4 expression levels affect synaptic connectivity, we used the rabies virus-mediated monosynaptic tracing technique, a method that allows an efficient analysis of functional presynaptic partners (Wickersham et al., 2007a). For that, cortical neurons were transfected with a retroviral vector encoding the EnvA-receptor TVA, the rabies virus glycoprotein G (which is responsible for retrograde transport of the virus across synapses), and the fluorescent reporter DsRedExpress2 (Fig. 5A). Neurons transfected with this vector are susceptible to subsequent infection by the glycoprotein G-deficient, eGFP-encoding EnvA-pseudotyped rabies virus (RABV) and capable of retrograde transfer of the virus to all immediate presynaptic partners (Deshpande et al., 2013; Wickersham et al., 2007a) (Fig. 5B). The schematics in Fig. 5B,C illustrate the strategy and the timeline for monosynaptic tracing of presynaptic partners of neurons *in vitro*. Transfection of the G- and TVA-encoding plasmid together with either pCAG-DsRed or pCAG-miRLRP4-DsRed followed by RABV infection 7 days later resulted in the appearance of double reporter-positive neurons (starter cells) at low density, indicating that these cells had received both the plasmids and the virus (yellow cells; Fig. 5D, white arrows). Green cells expressing only eGFP represent cells with transsynaptic transmission of RABV from the starter neurons (Fig. 5D). Because transsynaptic transmission of the RABV requires synaptic contacts, the green cells are presynaptic to the starter cells ($DsRed^{+}/GFP^{+}$, yellow). Analysis of the eGFP-labeled cells demonstrated that the number of direct presynaptic partners of LRP4 knockdown neurons was significantly lower compared with control neurons (Fig. 5E). This indicates that the LRP4 knockdown-mediated reduction of synapse-like specializations and spines is accompanied by a reduced number of synapses.

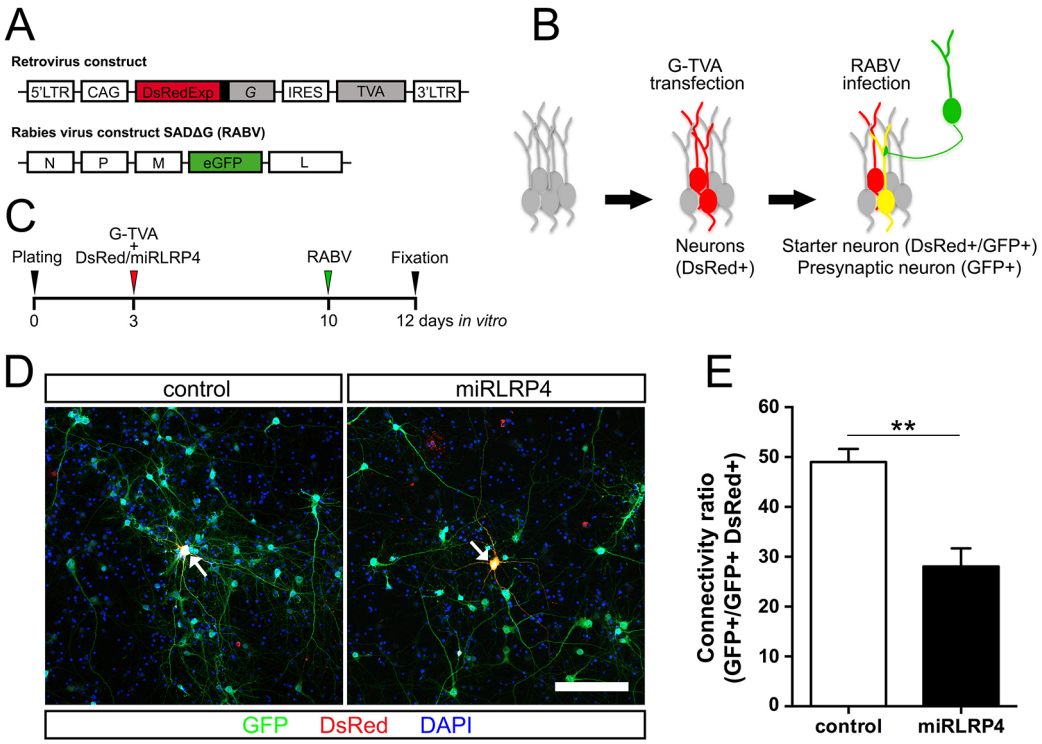

Fig. 5. Knockdown of LRP4 in cortical neurons decreases the number of presynaptic partners. (A) Schematic of the RABV and Glyco-TVA constructs used to investigate the number of functional presynaptic connections after LRP4 knockdown. (B) Experimental design for tracing monosynaptic connections in cortical neuronal cultures via consecutive delivery of G- and TVA-expression construct and RABV. (C) Timeline of the experimental protocol. (D) Representative examples of cortical neurons from E14 embryos at DIV12 co-transfected with the G/TVA-encoding vector and either pCAG-DsRed (left) or pCAG-miRLRP4-DsRed (right), followed by RABV infection. Arrows indicate double-transduced starter neurons. Note that the number of GFP^{+} cells surrounding a GFP^{+}/RFP^{+} (starter) neuron is lower upon knockdown of LRP4. (E) Ratio of RABV-traced cells versus GFP/RFP double-positive starter neurons in control and knockdown conditions. The number of direct presynaptic partners is reduced by approximately 40% in neurons after knockdown of LRP4. Data show mean±s.d. from three independent experiments. $^{**}P<0.01$ (unpaired *t*-test with Welch's correction). Scale bar: 100 µm.

Development (2017) 144, 4604-4615 doi:10.1242/dev.150110

Agrin is required for the LRP4-mediated effect on dendritic development and synapse formation

At the neuromuscular junction, LRP4 is the receptor for the motoneuron-derived extracellular matrix proteoglycan agrin (Kim et al., 2008; Zhang et al., 2008). We hypothesized that agrin might also regulate the effect of LRP4 on dendritic morphology in cultured CNS neurons. As a first step, we examined whether LRP4 influences the distribution of agrin in cultured neurons. To this end, we co-transfected cultured cortical neurons with pCAG-DsRed and pSYN-LRP4 on DIV2 and subsequently with pSYN-GFP:actin and a vector in which the transmembrane form of agrin was expressed under the control of the synapsin promoter (pSYN-TMagrin) on DIV3. Analysis of the sites of axon-dendrite contact by confocal microscopy revealed that agrin was highly concentrated at contact sites between dendrites of neurons overexpressing LRP4 and axons overexpressing TM-agrin (Fig. 6A). In contrast, neurons overexpressing TM-agrin did not concentrate agrin immunoreactivity at the sites of contact to neurons in which LRP4 had been knocked down (Fig. 6B). These results suggest that LRP4 affects the distribution of TM-agrin in neurons and are consistent with the hypothesis that LRP4 is involved in aggregating TM-agrin at CNS synapses.

We next analyzed the effect of LRP4 overexpression on cortical neurons in the presence or absence of functional blocking antibodies for agrin (Fig. 6C). These polyclonal antibodies were generated against a 95 kDa C-terminal fragment of mouse agrin (Eusebio et al., 2003), which has been shown to be responsible for LRP4 binding and acetylcholine receptor aggregation at the NMJ. Neurons overexpressing LRP4 had reduced numbers of spines (Fig. 6D) and primary dendrites (Fig. 6E), and increased dendritic length (Fig. 6F) in the presence of anti-agrin antibodies, compared with neurons overexpressing LRP4 in the presence of the preimmune serum. Thus, addition of anti-agrin antibodies reversed the effect of LRP4 overexpression (for control values see white bars in Fig. 6D-F), suggesting that agrin is involved in the LRP4 overexpression-mediated phenotype of CNS neurons *in vitro*.

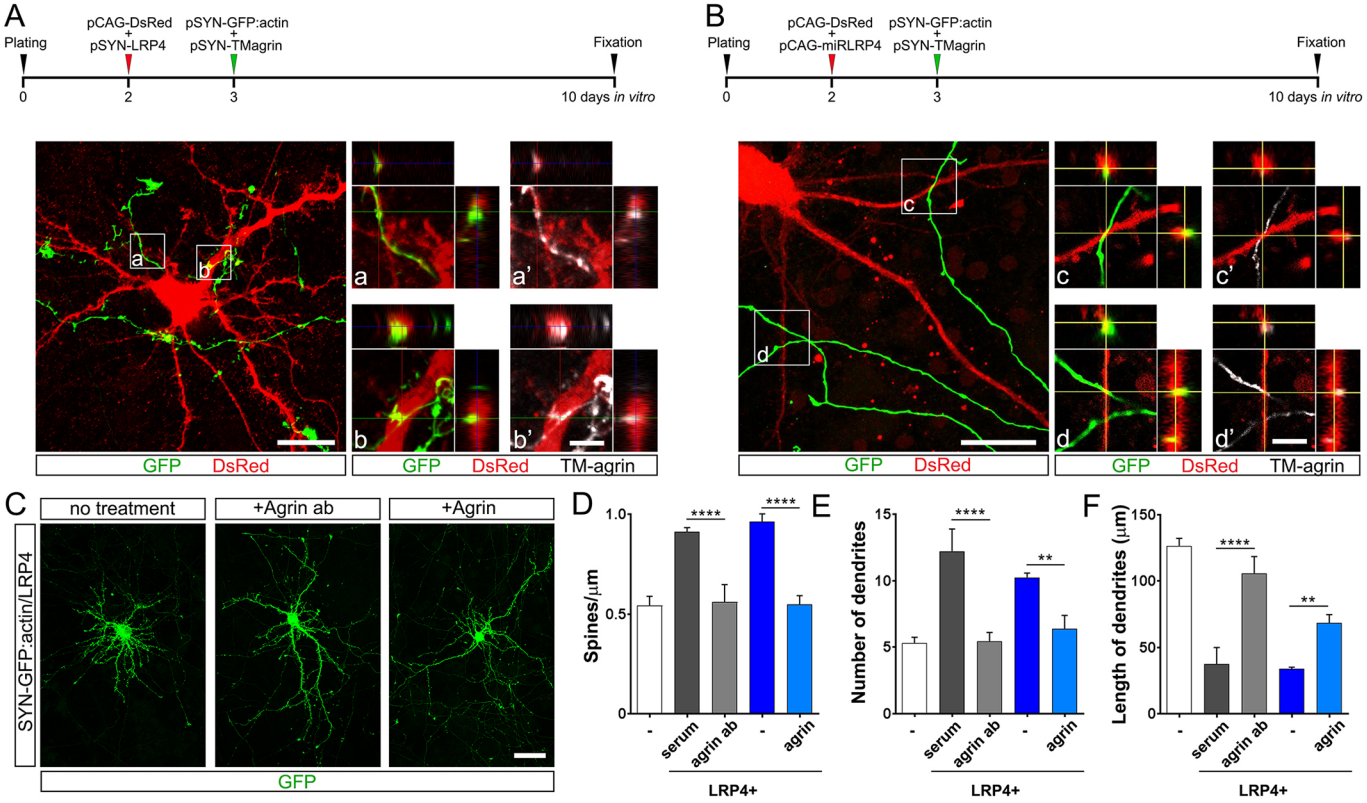

Fig. 6. Colocalization and functional interaction of LRP4 and agrin on dendrites *in vitro*. (A) Representative example of E14 cortical neurons sequentially co-transfected with pCAG-DsRed and pSYN-LRP4 on DIV2 (red) and pSYN-GFP:actin and pSYN-TMagrin on DIV3 (green). Note that TM-agrin is concentrated at contact sites between dendrites overexpressing LRP4 and axons overexpressing TM-agrin (insets a,b and a′,b′ represent orthogonal projections), indicating that LRP4 and TM-agrin from two different cells might interact. (B) Representative example of E14 cortical neurons sequentially co-transfected with pCAG-miRLRP4-DsRed on DIV2 (red) and pSYN-GFP:actin and pSYN-TMagrin on DIV3 (green). Note that TM-agrin appears not to be concentrated at contact sites between dendrites of neurons in which LRP4 expression has been knocked down and axons overexpressing TM-agrin (insets c,d and c′,d′ represent orthogonal projections). (C) Representative examples of dissociated cells from E14 cortex co-transfected with pSYN-GFP:actin and pSYN-LRP4. Neurons were treated with the soluble C-terminal 125 kDa (A4B8) chicken agrin fragment (right) or cultured in the presence of rabbit anti-agrin antibodies (middle). Note that both the presence of anti-agrin antibodies as well as the presence of the soluble agrin fragment ameliorates the dendritic phenotype caused upon LRP4 overexpression. (D-F) Quantifications of the density of spines (D), number of primary dendrites (E) and length of primary dendrites (F) in cortical neurons overexpressing LRP4 after treatment with the soluble C-terminal agrin fragment (light blue bars) or with anti-agrin antibodies (light gray bars). The bar labeled 'serum' refers to neurons sequentially transfected with the SYN-GFP:actin and the pSYN-LRP4 vectors (as shown in C) and cultured in the presence of the corresponding preimmune serum. Note that treatment with either the antibodies or with soluble agrin significantly decreased the density of spines (D) and the number of primary dendrites (E), and increased the dendritic length (F) compared with transfected neurons in the absence of agrin or the presence of preimmune serum. Data show mean±s.d. from three independent experiments, n=10 neurons per condition/experiment. $^{**}P<0.01$, $^{****}P<0.0001$ (one-way ANOVA with Tukey's post-hoc test). Scale bars: 50 µm (C); 25 µm (A,B, main panels); 10 µm (Aa-Ab′,Bc-Bd′).

Development (2017) 144, 4604-4615 doi:10.1242/dev.150110

The effect of anti-agrin antibodies on dendritic growth suggested that an interaction of LRP4 with TM-agrin might be necessary for the formation of a normal dendritic arbor. To test this further, we investigated whether a soluble C-terminal fragment of an agrin isoform (A4B8), which is able to bind to LRP4 but is not anchored to the cell membrane or the extracellular matrix, interferes with the effect of LRP4 expression in cortical neurons. To this end, we analyzed the spine density, number of dendrites and dendritic length in embryonic neurons upon LRP4 overexpression in the presence or absence of the C-125 fragment of chick agrin (Pevzner et al., 2012; Tsim et al., 1992). Cultures were fixed 3-4 days after transfection and agrin addition, and morphometric analysis was performed as described above. The presence of the soluble agrin fragment led to a decrease in spine density (Fig. 6D) and number of primary dendrites (Fig. 6E), as well as an increase in dendritic length (Fig. 6F) in cortical neurons overexpressing LRP4. Thus, soluble agrin reversed the effect of LRP4 overexpression on dendritic growth and spine formation (for control values see white bars in Fig. 6D-F) mimicking the effect of the anti-agrin antibodies. This further supports that an interaction of LRP4 with TM-agrin is required for normal dendritic and spine development in cortical neurons. Furthermore, the similar effects of the anti-agrin antibodies and the soluble agrin fragment demonstrate that a membrane association of agrin is required for the LRP4-mediated changes in dendritic morphology and spine density in CNS neurons.

Neuronal LRP4 regulates dendritic development and spine formation in neurons *in vivo*

To investigate whether the altered dendritic morphology and synapse number observed in cultured embryonic neurons after knockdown of LRP4 could also be observed *in vivo*, we performed *in utero* electroporation of the LRP4 miRNAs. To this end, the SYN-miRLRP4-DsRed plasmid was co-electroporated with the SYN-GFP:actin vector into the hippocampus and cortex of embryonic day (E) 14.5 embryos. Electroporation of the pSYN-DsRed plasmid together with the pSYN-GFP:actin vector was used as control. This protocol allowed us to target groups of neurons in layers II-IV of the cortex and CA1 area of the hippocampus (see Fig. 7A for a schematic of the vectors and Fig. 7B for the injection sites and the timeline of the experiments). Dendritic morphology and spines were analyzed by confocal microscopy of brain sections from postnatal day (P) 21 animals (Fig. 7C,E). To investigate the effect of LRP4 knockdown on spines we analyzed their density on dendrites of electroporated neurons. Quantifications revealed that expression of miRLRP4 in embryonic neurons *in vivo* resulted in an approximately 40% decrease in the density of dendritic spines in cortical (Fig. 7D) and hippocampal (Fig. 7F) neurons. These results demonstrate a role for LRP4 in establishing or maintaining synapses in neurons in the cortex and CA1 region of the hippocampus.

Finally, to investigate the effect of LRP4 knockdown on dendritic development *in vivo*, we performed a morphometric analysis of single electroporated cells. Within cortical areas, the compact distribution of electroporated neurons did not allow us to identify single cells (Fig. 7C). However, only a few cells within the hippocampus were electroporated and could be unambiguously identified in coronal sections (Fig. 7E). Fig. 7G shows examples of individual CA1 hippocampal neurons electroporated with either the control plasmids (Fig. 7G, left) or the miRLRP4 plasmid (Fig. 7G, right) and traced with the Simple Neurite Tracer (Longair et al., 2011). Sholl analysis revealed that control hippocampal neurons had a greater number of intersections in a radius between 10 and 500 µm from the cell body compared with neurons in which LRP4 expression was reduced (Fig. 7H). Moreover, morphometric analysis of transfected cells revealed that reduced LRP4 expression significantly decreased the number of primary dendrites in embryonic hippocampal neurons (Fig. 7I) whereas their average dendritic length was not noticeably altered (data not shown). Because the electroporation procedure was not ideal for targeting neurons located in the CA3 area of the hippocampus, we were not able to determine whether this region would also be affected by LRP4 knockdown. However, we observed that cultured neurons from CA3 and CA1/dentate gyrus areas, which can be identified as CTIP2 $(BCL11B)^{-}$ and $CTIP2^{+}$ cells, respectively, are all immunoreactive for LRP4 (Fig. S5), suggesting that neuronal LRP4 might play an important role in all the areas of the hippocampus.

DISCUSSION

LRP4 has a fundamental role during formation, maintenance and regeneration of the NMJ (for a review, see Tintignac et al., 2015). Moreover, cumulative evidence indicates that LRP4 plays crucial roles in synaptic function in the CNS (Kim et al., 2008; Wu et al., 2012; Zhang et al., 2008). However, the molecular mechanisms regulating these functions are still mostly unknown. A recent study indicated that, in *Drosophila*, presynaptic expression of LRP4 regulates synapse number (Mosca et al., 2017). Studies in LRP4-deficient mice rescued from perinatal death by re-expression of LRP4 in the neuromuscular system, as well as mice with a selective loss of the intracellular and the transmembrane domains showed a significantly decreased density of dendritic spines in the CA3-hippocampal region, but had no gross anatomical abnormalities in the prenatal and adult hippocampus, cortex and cerebellum (Pohlkamp et al., 2015; Gomez et al., 2014). In addition, *Lrp4* mRNA is present in the neocortex, hippocampus, cerebellum and olfactory bulb (Sun et al., 2016; Lein et al., 2007; Tian et al., 2006). A recent study (Sun et al., 2016) reported that in adult mice β-galactosidase expression driven by the endogenous *Lrp4* promoter is mostly detectable in astrocytes, which is in concordance with our data showing that LRP4 levels, detected by western blotting, are higher in astrocytes than in neurons (Fig. 1D). Moreover, it was demonstrated that the activation of astroglial LRP4 by neuronal agrin induced the release of ATP, which modulates the synaptic activity of hippocampal pyramidal neurons (Sun et al., 2016). Consistently, mice with a conditional knockout for astroglial *Lrp4* mRNA exhibited reduced glutamatergic synaptic transmission in neurons from the CA3 region. However, depletion of LRP4 expression in astrocytes did not lead to a decreased density of dendritic spines in the hippocampus (Sun et al., 2016), suggesting that other cell sources of LRP4 (i.e. neurons, oligodendrocytes or microglia) play additional roles in the CNS. In our study, we revealed that reduced LRP4 expression specifically in cortical and hippocampal neurons *in vitro* and *in vivo* led to a reduced density of spines and dendrite-associated synapse-like specializations, including bassoon- and synaptobrevin2-positive puncta. Accordingly, increased LRP4 expression in cultured CNS neurons resulted in an increase in the number of spines. As the experiments reported in our study affected LRP4 expression only in neurons (due to the neuron-specific synapsin promoter), the altered spine density that we observed must be caused by changes in neuronally expressed LRP4. Moreover, using a rabies virus-mediated monosynaptic tracing technique (Wickersham et al., 2007a), we demonstrated that the decreased number of synapse-like specializations and dendritic spines mediated by the expression of LRP4 miRNAs is paralleled by a decrease in the number of synaptic inputs as well, and therefore functional synapses.

Development (2017) 144, 4604-4615 doi:10.1242/dev.150110

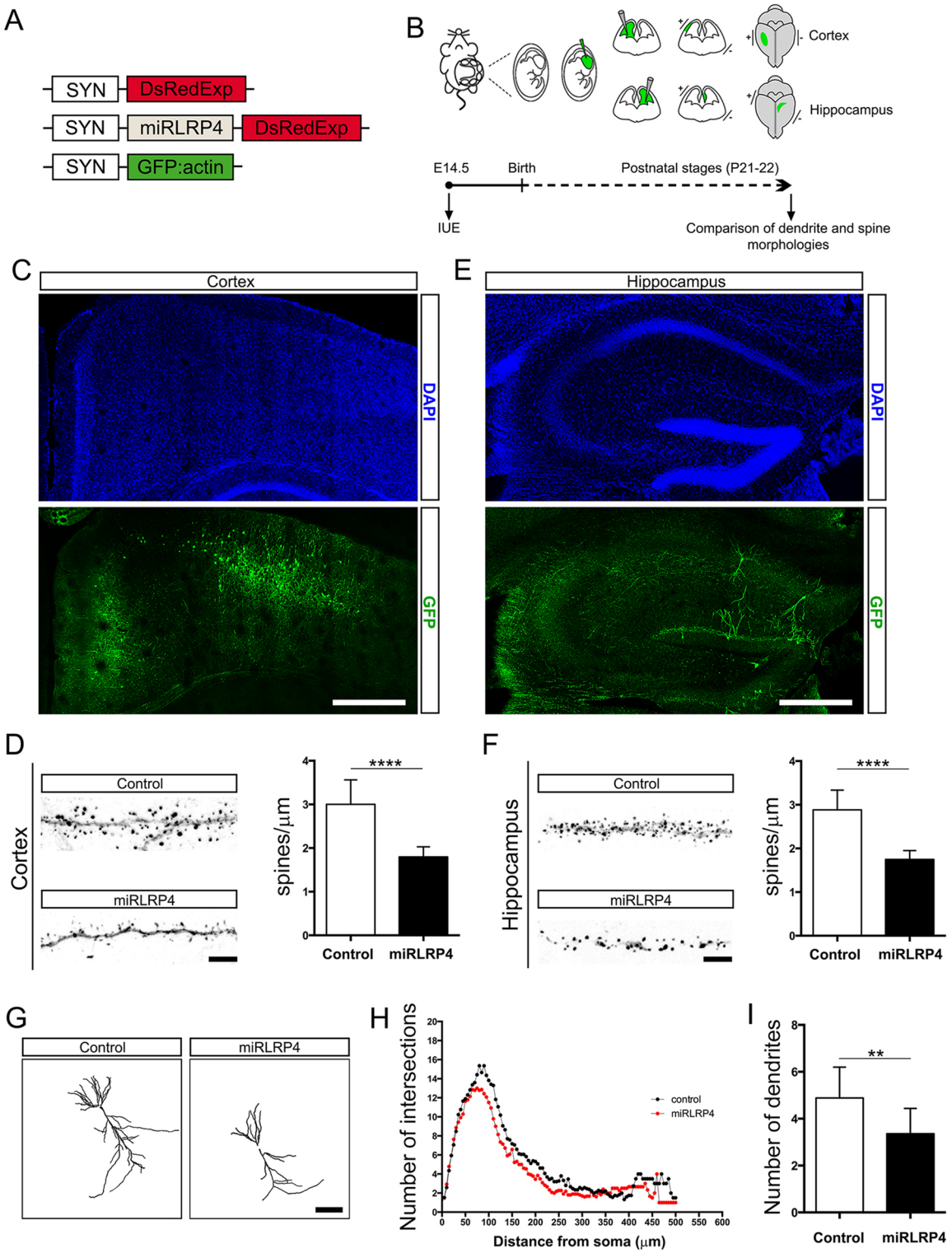

Fig. 7. Knockdown of LRP4 *in vivo* by *in utero* electroporation reduces dendritic number and spine density. (A) Constructs encoding DsRed, GFP:actin and miRLRP4 (miR1232 and miR1544 in tandem array) used to reduce LRP4 expression *in vivo*. DsRed, GFP:actin and miRLRP4 expression were under the control of the SYN promoter. (B) Schematic of the *in utero* electroporation technique, the injection sites used to target specific brain areas and the timeline of the experimental protocol. (C,E) Representative examples of the electroporation sites in cortex (C) and hippocampus (E) of P21 mice. (D,F) High-resolution analysis of dendritic segments from cortical (D) and CA1 hippocampal (F) neurons electroporated with either the control or the miRLRP4 plasmid. The GFP:actin fluorescence revealing spines is shown on the left side of each panel. Quantification of the density of spines per dendritic length in electroporated cortical (D) and hippocampal (F) neurons is shown on the right side of each panel. (G) Representative examples of CA1 hippocampal neurons electroporated with either the control or the miRLRP4 plasmid and traced with the ImageJ Simple Neurite Tracer plugin. (H) Quantification of the tracings shown in G by Sholl analysis shows a reduced number of intersections in neurons electroporated with miRLRP4. The radius interval between the circles was 10 µm per step ranging from 0 to 500 µm from the center of the neuronal soma. (I) Quantification of the number of primary dendrites of CA1 hippocampal neurons. Data represent mean±s.d. from three independent experiments. ***P*<0.01, *****P*<0.0001 (unpaired *t*-test with Welch's correction). Scale bars: 500 µm (C,E); 5 µm (D,F); 50 µm (G).

Development (2017) 144, 4604-4615 doi:10.1242/dev.150110

Hippocampal and cortical neurons in culture also responded to reduced LRP4 expression by changes in dendritic morphology. Fewer but longer dendritic processes were generated when the density of synapse-like specializations was decreased. Overexpression of LRP4 in these neurons had the opposite effect, i.e. more but shorter dendrites extended from the soma with a concomitant increase in synaptic density. Moreover, we observed that knockdown of neuronal LRP4 also led to a decrease in the number of dendritic branches in the CA1 area of the hippocampus *in vivo*. Interestingly, the effect of LRP4 knockdown and overexpression on dendrite numbers disappears in cultured neurons over time (Fig. 3). This could explain why changes in dendritic morphology were not previously detected in adult LRP4-deficient brains (Gomez et al., 2014; Pohlkamp et al., 2015; Sun et al., 2016). However, changes in dendrite length remain evident after 21 days of maturation *in vitro*, suggesting that LRP4 levels would still have a long-term impact on neuronal arbor.

Previous studies have shown that dendritogenesis is a highly dynamic process that is influenced by synaptic activity as well as by signals from the immediate environment (for reviews, see Cheng and Poo, 2012; Dong et al., 2015). The opposite effects of LRP4 overexpression and knockdown on the number of primary dendrites, their length and on spine/synapse density suggest that all these effects might be mechanistically linked. One possibility is that the increase in the dendritic length observed in neurons with reduced levels of LRP4 is a consequence of the decrease in synaptic density. However, this is unlikely to be the case as we observed that the effect of LRP4 on dendritic arborization takes place before the development of synaptic specializations (Fig. 3). Another possibility is that LRP4 regulates the dynamics of cytoskeleton assembly, as rearrangements of cytoskeletal architecture is crucial for both dendrite morphogenesis (Flynn, 2013) and development of presynaptic terminals (Dent et al., 2011). Supporting this hypothesis, we observed that LRP4 overexpression results in a decreased mobility of dendrite terminals, blocking both extension and retraction of growing dendrites (Fig. S3). Accordingly, we detected immunoreactivity for LRP4 in dendritic growth cones. However, further studies are needed to determine the molecular signals regulating these processes.

At the NMJ, the interaction of LRP4 with agrin is crucial for synaptogenesis (Tintignac et al., 2015). In CNS neurons, we show that anti-agrin antibodies or addition of a soluble C-terminal agrin fragment reversed the effects of LRP4 overexpression. As both treatments would interfere with the TM-agrin-LRP4 interaction either by blocking agrin binding to LRP4 (antibodies) or by competing with the ligand-binding site of LRP4 (soluble agrin fragment), these results implicate TM-agrin as one potential binding partner for LRP4 in the CNS. Thus, TM-agrin-LRP4 interactions might shape dendritic morphology and induce the formation of synapses in cultured neurons of the CNS. This hypothesis is further strengthened by our observation that agrin accumulated at contact sites between dendrites of neurons with increased LRP4 expression and axons overexpressing agrin, whereas agrin did not aggregate at contact sites with neurons in which LRP4 expression was reduced. Interestingly, neurons in the brain of agrin$^{-/-}$ mice, in which the perinatal lethality has been rescued by motoneuron-specific expression of agrin, also develop fewer synapses and shorter dendrites (Ksiazek et al., 2007).

Although our study focused on cortical and hippocampal neurons, LRP4 has a widespread expression pattern in the CNS, including astrocytes and neuronal populations outside of the forebrain, such as the cerebellum and the olfactory bulb (Tian et al., 2006; data not shown). It is therefore conceivable that LRP4 generally regulates dendritogenesis and synapse formation in many regions of the brain beyond the cerebral cortex and hippocampus. Our study provides the first indications of a function for LRP4 in dendrite and synapse formation in developing forebrain neurons, opening up avenues for elucidating the underlying molecular mechanisms in these and other regions of the CNS. Our results also suggest that at the molecular level, synaptogenesis at the NMJ and in the CNS are more similar than previously anticipated.

MATERIALS AND METHODS

Animals and ethical approval

Use and care of animals was approved by German authorities and according to national law (TierSchG). C57BL/6J wild-type mice were bred in the animal facility of the Institute of Physiology of LMU Munich. The day of the vaginal plug was considered E0. Mice with a targeted deletion of the *Musk* gene have been described previously (DeChiara et al., 1996). For *in utero* electroporation, animals were operated upon as approved by the Regionspräsidium Karlsruhe (Baden Württemberg, Germany) under license number 35-9185.81/G-28/16. All experimental procedures were performed in accordance with German and European Union guidelines.

Neuronal cultures, transfection, cell treatments and immunocytochemistry

Primary cultures of embryonic cortical and hippocampal neurons were prepared as described (Brewer et al., 1993). Transfections with Lipofectamine 2000 (Invitrogen) were performed on DIV2-3 according to the manufacturer's instructions. The number of transfected cells was in the range of 2% and the efficiency was similar for each of the vectors used. One day after transfection, neurons were treated with 16 U chick agrin (C-terminal 125 kDa fragment isoform A4B8; Pevzner et al., 2012) or with 0.6 µl rabbit polyclonal anti-agrin antibody (serum 204; Eusebio et al., 2003) in 0.5 ml culture medium. We observed no effect of the antibodies on cell death and number of neurons and non-neuronal cells in the cultures. Fixation and staining of the neuronal cultures was performed as described (Zhang et al., 2015; see supplementary Materials and Methods for details on antibodies).

Time-lapse imaging of dissociated cortical neurons was performed as previously described (Costa et al., 2011). For further details, see the supplementary Materials and Methods.

Rabies virus and G-TVA construct

The construct encoding for DsRedExpress2, the RABV glycoprotein (G) and the TVA800 (the GPI-anchored form of the TVA receptor), designed as CAG-DsRedExpress2-2A-G-IRES2-TVA (i.e. G-TVA construct), as well as the construction of the G gene-deleted and EnvA-pseudotyped *GFP*-expressing RABV (SADΔG-GFP) have been described previously (Wickersham et al., 2007a,b). Cells that express the G-TVA can be infected with EnvA-pseudotyped SADΔG-GFP and allow for transsynaptic transmission into all presynaptic neurons synaptically innervating the transfected and infected neuron. The connectivity with presynaptic neurons was determined by counting the double-fluorescent cells (GFP$^+$/DsRED$^+$) and the RABV-only single-positive cells (GFP$^+$). Results were expressed as connectivity ratio, representing the number of GFP-positive cells per GFP- and DsRed-double positive cells as described (Wickersham et al., 2007a).

cDNA constructs

For overexpression of LRP4 in cortical and hippocampal neurons, the full-length coding sequence of mouse *Lrp4* from pCMV-*Lrp4* (commercially obtained from the German Center of Genome Research, Source BioScience, Nottingham, UK) was cloned into the pcDNA3.1(−) vector, in which the cytomegalovirus (CMV) promoter was replaced by the neuron-specific synapsin (SYN) promoter (Kügler et al., 2001). For knockdown of LRP4 by RNA interference, four different synthetic microRNA (miRNA) sequences (BlockIT Invitrogen) targeting the open reading frame and 3′ UTR of *Lrp4* mRNA were individually cloned into the pcDNA6.2-GW vector. The targeted cDNA sequences for miRNAs were: LRP4 miR_1 (miR1232): 5′-TGAGGAGAACTGCAATGTTAA-3′; LRP4 miR_2 (miR1544): 5′-

Development (2017) 144, 4604-4615 doi:10.1242/dev.150110

CGAGTACACGCTGCTACTGAA-3′; LRP4 miR_3 (miR6854): 5′-CTTT-CAAAGACTGGCTCAACA-3′; LRP4 miR_4 (miR7072): 5′-CATTAGCT-TCATGCTCCTTTA-3′.

Western blotting (see supplementary Materials and Methods) and quantitative analysis of LRP4 protein levels in HEK293 cells transiently transfected with full-length mouse LRP4 cDNA and subsequent transfection with the miRNAs revealed that miR1232 and miR1544 were the most efficient in reducing LRP4 protein levels (Fig. S2A). For knockdown of LRP4 by RNA interference *in vitro* and *in utero*, the miR1232 and miR1544 microRNAs were expressed as tandems with the DsRed cDNA sequence and cloned in an expression vector under the control of either the CAG or the neuron-specific synapsin (SYN) promoter (CAG/SYN-miRLRP4-DsRed), respectively. This plasmid was co-electroporated with the SYN-GFP:actin vector, in order to visualize spines and small protrusions. As control for the electroporation we used the pSYN-DsRed plasmid together with the pSYN-GFP:actin vector.

For overexpression of TM-agrin in neurons, the coding sequence of mouse TM-agrin was cloned into a pMES plasmid in which the CMV promoter was replaced by the SYN promoter. As control for the transfections we used the pSYN-GFP:actin vector (generously provided by Fransisco G. Scholl; Gascón et al., 2008) and the pCAG-DsRed (Heinrich et al., 2014). All constructs were verified by DNA sequencing and were produced under endotoxin-free conditions (Invitrogen EndoFree Plasmid Maxi Kit).

Electrophysiological recordings

Whole-cell patch-clamp analysis of hippocampal neurons in culture after transfection with control vector or with miRLRP4 cDNA were used to record spontaneous mEPSCs. For further details, see supplementary Materials and Methods.

In utero electroporation

In utero electroporation of E14.5 timed pregnant mice (C57/Bl6; commercially obtained by Janvier Labs, Le Genest-Saint-Isle, France) was performed as previously described (Pacary et al., 2012). Specifically, pregnant mice were anesthetized with isoflurane (induction, 3%; surgery, 1.5%). The analgesic was applied directly after the anesthesia by subcutaneously injecting Carprofen (5 mg/kg). The uterine horns were exposed by Cesarean section and sterile, pre-warmed saline was repeatedly applied during the operation to keep the intestines moist. Animals were kept on a heating pad during the whole process of operation. Plasmids were mixed with Fast Green (2.5 mg/µl, Sigma) and 2 µl (at a concentration of 1 µg/µl) were injected into the lateral ventricle by use of a glass capillary under illumination of the uterine horns by a halogen cold light. DNA was electroporated into the hippocampus with five electrical pulses (amplitude, 40 V; duration, 50 ms; intervals, 1 s). During the pulsing the electrodes were swept from 0° to 45° for targeting the CA1 and CA3 regions, respectively. After electroporation, the uterine horns were carefully repositioned into the abdominal cavity, which was then filled with pre-warmed saline. The abdominal muscle and skin incisions were closed with surgical sutures with medical sewing equipment. Animals were left to recover in a clean cage and embryos allowed to continue their development. At P21, mice were anesthetized with ketamine and xylazine, and then transcardially perfused with PBS (pH 7.4) and fixative containing 4% paraformaldehyde in PBS. Brains were dissected and post-fixed overnight at 4°C. Brains were then sectioned at 100 µm thickness using a VT1200s vibratome (Leica). Sections were treated with 0.3% Triton X-100 in PBS (PBT) and non-specific staining was blocked with 1% bovine serum albumin and 2% normal donkey serum in PBT. All specimens were analyzed using a Zeiss LSM710 or a LSM780 laser-scanning microscope as detailed above. Digital processing of entire images, including adjustment of brightness and contrast, was performed using Photoshop CS3 (Adobe).

Image collection and quantitative analysis

Dendritic number and length quantifications

The number of primary dendrites emerging from the soma was manually counted. Axons were excluded from the analysis, as they can be distinguished morphologically from the dendrites (axons are thinner, longer, without spines). In addition, to facilitate the identification of dendrites, in most cases we performed immunostaining for MAP2 (labeling dendrites) and for Tau (MAPT; labeling axons). The dendritic length in microns was determined using the Zen2009 software (Zeiss) and the ImageJ Simple Neurite Tracer plugin (Longair et al., 2011) in cortical and hippocampal neurons using the images obtained with a LSM710 laser-scanning confocal or Axio Observer Z1 epifluorescence microscope (Carl Zeiss). The dendritic length in the graphs represents the average length of all the primary dendrites of each neuron (e.g. in a neuron with five primary dendrites the length of all of them was measured starting from the neuron soma and ending at the most distal point of the dendrite and we then calculated the average).

For the *in utero* electroporation, dendritic branching was analyzed using the Simple Neurite Tracer and the ImageJ plugin for Sholl analysis (Ferreira et al., 2014).

Spines and synapse-like specializations

High-resolution *z*-stacks of dendrites from cortical and hippocampal neurons were collected with a 40× lens and a 2× digital zoom factor (thickness of optical sections: 0.4-1 µm). Spines were morphologically identified in the transfected neurons as short GFP^+ protrusions emerging from the dendrites. Spine density was manually determined along dendritic segments. The density of bassoon-, synaptobrevin-2- and PSD95-positive puncta was also manually determined.

In all the aforementioned quantifications, experimenter was blind to the conditions analyzed.

Statistical analysis

Results are presented as mean±s.d. Significance was calculated with GraphPad Prism 5 (GraphPad Software) using a one-way ANOVA test with Dunnett's post-hoc test. Analysis of transfected neurons treated with soluble agrin and anti-agrin antibodies was performed using a one-way ANOVA test with Tukey's post-hoc test. For the *in utero* electroporation experiments and the experiments with the rabies virus, we used an unpaired *t*-test with Welch's correction. $P<0.05$ was set as the level of statistical significance.

Acknowledgements

We would like to thank Katja Peters and Martina Bürkle for expert technical assistance; Aditi Desphande, Antigona Ulndreaj, John Bixby, Fritz Rathjen and Elisa Murenu for insightful comments and for critically reading and improving the manuscript; Fritz Rathjen for the *Lrp4*$^{-/-}$ mouse muscle tissue; Magdalena Götz for constant support and encouragement; and Wilko Altrock for generously providing anti-bassoon antibodies. Parts of the results shown in Figs 1-6 in this paper are reproduced from the PhD thesis of Andromachi Karakatsani (Karakatsani, 2015).

Competing interests

The authors declare no competing or financial interests.

Author contributions

Conceptualization: A.K., S.G., S.K.; Methodology: A.K., N.M., S.U., S.G., S.K.; Formal analysis: A.K., G.K., Y.Z.; Investigation: A.K., S.G., S.K.; Resources: A.S., A.G., K.-K.C., M.A.R., B.B.; Data curation: A.K., S.G., S.K.; Writing - original draft: A.K., S.G., S.K.; Writing - review & editing: A.K., C.R.A., S.G., S.K.; Visualization: A.K., S.G., S.K.; Supervision: S.G., S.K.; Project administration: S.G., S.K.; Funding acquisition: S.K.

Funding

The work was supported by grants from the Deutsche Forschungsgemeinschaft (DFG; KR1039-11-1 to S.K., SFB870 to A.G. and K.-K.C., and CRC1080 to B.B.) and the European Research Council (ERC-StG-311367 to C.R.A.). N.M. was supported by a Long-Term Fellowship of the Human Frontier Science Program.

Supplementary information

Supplementary information available online at
http://dev.biologists.org/lookup/doi/10.1242/dev.150110.supplemental

References

Brewer, G. J., Torricelli, J. R., Evege, E. K. and Price, P. J. (1993). Optimized survival of hippocampal neurons in B27-supplemented Neurobasal, a new serum-free medium combination. *J. Neurosci. Res.* **35**, 567-576.

Caceres, A., Banker, G., Steward, O., Binder, L. and Payne, M. (1984). MAP2 is localized to the dendrites of hippocampal neurons which develop in culture. *Brain Res.* **315**, 314-318.
Cheng, P.-L. and Poo, M.-M. (2012). Early events in axon/dendrite polarization. *Annu. Rev. Neurosci.* **35**, 181-201.
Costa, M. R., Ortega, F., Brill, M. S., Beckervordersandforth, R., Petrone, C., Schröder, T., Götz, M. and Berninger, B. (2011). Continuous live imaging of adult neural stem cell division and lineage progression *in vitro*. *Development* **138**, 1057-1068.
DeChiara, T. M., Bowen, D. C., Valenzuela, D. M., Simmons, M. V., Poueymirou, W. T., Thomas, S., Kinetz, E., Compton, D. L., Rojas, E., Park, J. S. et al. (1996). The receptor tyrosine kinase MuSK is required for neuromuscular junction formation *in vivo*. *Cell* **85**, 501-512.
Dent, E. W., Merriam, E. B. and Hu, X. (2011). The dynamic cytoskeleton: backbone of dendritic spine plasticity. *Curr. Opin. Neurobiol.* **21**, 175-181.
Deshpande, A., Bergami, M., Ghanem, A., Conzelmann, K.-K., Lepier, A., Götz, M. and Berninger, B. (2013). Retrograde monosynaptic tracing reveals the temporal evolution of inputs onto new neurons in the adult dentate gyrus and olfactory bulb. *Proc. Natl. Acad. Sci. USA* **110**, 1152-1161.
Dong, X., Shen, K. and Bülow, H. E. (2015). Intrinsic and extrinsic mechanisms of dendritic morphogenesis. *Annu. Rev. Physiol.* **77**, 271-300.
Eusebio, A., Oliveri, F., Barzaghi, P. and Ruegg, M. A. (2003). Expression of mouse agrin in normal, denervated and dystrophic muscle. *Neuromuscul. Disord.* **13**, 408-415.
Ferreira, T. A., Blackman, A. V., Oyrer, J., Jayabal, S., Chung, A. J., Watt, A. J., Sjöström, P. J. and van Meyel, D. J. (2014). Neuronal morphometry directly from bitmap images. *Nat. Methods* **11**, 982-984.
Fischer, M., Kaech, S., Knutti, D. and Matus, A. (1998). Rapid actin-based plasticity in dendritic spines. *Neuron* **20**, 847-854.
Flynn, K. C. (2013). The cytoskeleton and neurite initiation. *Bioarchitecture* **3**, 86-109.
Gascón, S., Paez-Gomez, J. A., Diaz-Guerra, M., Scheiffele, P. and Scholl, F. G. (2008). Dual-promoter lentiviral vectors for constitutive and regulated gene expression in neurons. *J. Neurosci. Methods* **168**, 104-112.
Gomez, A. M., Froemke, R. C. and Burden, S. J. (2014). Synaptic plasticity and cognitive function are disrupted in the absence of Lrp4. *eLife* **3**, e04287.
Heinrich, C., Bergami, M., Gascón, S., Lepier, A., Viganò, F., Dimou, L., Sutor, B., Berninger, B. and Götz, M. (2014). Sox2-mediated conversion of NG2 glia into induced neurons in the injured adult cerebral cortex. *Stem Cell Rep.* **3**, 1000-1014.
Jones, E. G., Huntley, G. W. and Benson, D. L. (1994). Alpha calcium/calmodulin-dependent protein kinase II selectively expressed in a subpopulation of excitatory neurons in monkey sensory-motor cortex: comparison with GAD-67 expression. *J. Neurosci.* **14**, 611-629.
Karakatsani, A. (2015). LRP4 regulates dendritic arborization and synapse formation in the central nervous system. PhD thesis, Ludwig-Maximilians University. https://edoc.ub.uni-muenchen.de/20026/1/Karakatsani_Andromachi.pdf.
Kim, N., Stiegler, A. L., Cameron, T. O., Hallock, P. T., Gomez, A. M., Huang, J. H., Hubbard, S. R., Dustin, M. L. and Burden, S. J. (2008). Lrp4 is a receptor for Agrin and forms a complex with MuSK. *Cell* **135**, 334-342.
Ksiazek, I., Burkhardt, C., Lin, S., Seddik, R., Maj, M., Bezakova, G., Jucker, M., Arber, S., Caroni, P., Sanes, J. R. et al. (2007). Synapse loss in cortex of agrin-deficient mice after genetic rescue of perinatal death. *J. Neurosci.* **27**, 7183-7195.
Kügler, S., Meyn, L., Holzmüller, H., Gerhardt, E., Isenmann, S., Schulz, J. B. and Bähr, M. (2001). Neuron-specific expression of therapeutic proteins: evaluation of different cellular promoters in recombinant adenoviral vectors. *Mol. Cell. Neurosci.* **17**, 78-96.
Lein, E. S., Hawrylycz, M. J., Ao, N., Ayres, M., Bensinger, A., Bernard, A., Boe, A. F., Boguski, M. S., Brockway, K. S., Byrnes, E. J. et al. (2007). Genome-wide atlas of gene expression in the adult mouse brain. *Nature* **445**, 168-176.
Longair, M. H., Baker, D. A. and Armstrong, J. D. (2011). Simple Neurite Tracer: open source software for reconstruction, visualization and analysis of neuronal processes. *Bioinformatics* **27**, 2453-2454.
Mosca, T. J., Luginbuhl, D. J., Wang, I. E. and Luo, L. (2017). Presynaptic LRP4 promotes synapse number and function of excitatory CNS neurons. *eLife* **6**, e27347.
Pacary, E., Haas, M. A., Wildner, H., Azzarelli, R., Bell, D. M., Abrous, D. N. and Guillemot, F. (2012). Visualization and genetic manipulation of dendrites and spines in the mouse cerebral cortex and hippocampus using in utero electroporation. *J. Vis. Exp.* **65**, e4163.
Pevzner, A., Schoser, B., Peters, K., Cosma, N.-C., Karakatsani, A., Schalke, B., Melms, A. and Kröger, S. (2012). Anti-LRP4 autoantibodies in AChR- and MuSK-antibody-negative myasthenia gravis. *J. Neurol.* **259**, 427-435.
Pohlkamp, T., Durakoglugil, M., Lane-Donovan, C., Xian, X., Johnson, E. B., Hammer, R. E. and Herz, J. (2015). Lrp4 domains differentially regulate limb/brain development and synaptic plasticity. *PLoS ONE* **10**, e0116701.
Sloviter, R. S. and Nilaver, G. (1987). Immunocytochemical localization of GABA-, cholecystokinin-, vasoactive intestinal polypeptide-, and somatostatin-like immunoreactivity in the area dentata and hippocampus of the rat. *J. Comp. Neurol.* **256**, 42-60.
Sun, X.-D., Li, L., Liu, F., Huang, Z.-H., Bean, J. C., Jiao, H.-F., Barik, A., Kim, S.-M., Wu, H., Shen, C. et al. (2016). Lrp4 in astrocytes modulates glutamatergic transmission. *Nat. Neurosci.* **19**, 1010-1018.
Tian, Q.-B., Suzuki, T., Yamauchi, T., Sakagami, H., Yoshimura, Y., Miyazawa, S., Nakayama, K., Saitoh, F., Zhang, J.-P., Lu, Y. et al. (2006). Interaction of LDL receptor-related protein 4 (LRP4) with postsynaptic scaffold proteins via its C-terminal PDZ domain-binding motif, and its regulation by Ca/calmodulin-dependent protein kinase II. *Eur. J. Neurosci.* **23**, 2864-2876.
Tintignac, L. A., Brenner, H.-R. and Rüegg, M. A. (2015). Mechanisms regulating neuromuscular junction development and function and causes of muscle wasting. *Physiol. Rev.* **95**, 809-852.
Tsim, K. W. K., Ruegg, M. A., Escher, G., Kröger, S. and McMahan, U. J. (1992). cDNA that encodes active agrin. *Neuron* **8**, 677-689.
Weatherbee, S. D., Anderson, K. V. and Niswander, L. A. (2006). LDL-receptor-related protein 4 is crucial for formation of the neuromuscular junction. *Development* **133**, 4993-5000.
Wickersham, I. R., Finke, S., Conzelmann, K.-K. and Callaway, E. M. (2007a). Retrograde neuronal tracing with a deletion-mutant rabies virus. *Nat. Methods* **4**, 47-49.
Wickersham, I. R., Lyon, D. C., Barnard, R. J. O., Mori, T., Finke, S., Conzelmann, K.-K., Young, J. A. T. and Callaway, E. M. (2007b). Monosynaptic restriction of transsynaptic tracing from single, genetically targeted neurons. *Neuron* **53**, 639-647.
Wu, H., Lu, Y., Shen, C., Patel, N., Gan, L., Xiong, W. C. and Mei, L. (2012). Distinct roles of muscle and motoneuron LRP4 in neuromuscular junction formation. *Neuron* **75**, 94-107.
Yumoto, N., Kim, N. and Burden, S. J. (2012). Lrp4 is a retrograde signal for presynaptic differentiation at neuromuscular synapses. *Nature* **489**, 438-442.
Zhang, B., Luo, S., Wang, Q., Suzuki, T., Xiong, W. C. and Mei, L. (2008). LRP4 serves as a coreceptor of agrin. *Neuron* **60**, 285-297.
Zhang, Y., Lin, S., Karakatsani, A., Rüegg, M. A. and Kröger, S. (2015). Differential regulation of AChR clustering in the polar and equatorial region of murine muscle spindles. *Eur. J. Neurosci.* **41**, 69-78.